

# Effects of oxidation on fatigue crack initiation and propagation in an advanced disc alloy

R. Jiang<sup>1</sup>, N. Gao<sup>1</sup>, P. A. S. Reed<sup>1</sup>, D. Proppentner<sup>2</sup>, B. A. Shollock<sup>2</sup>, F. Farukh<sup>3</sup>, L. G. Zhao<sup>3</sup>

<sup>1</sup>Engineering Materials Research Group, Faculty of Engineering and Environments, University of Southampton, Southampton, SO17 1BJ, UK

<sup>2</sup>International Digital Laboratory, WMG, University of Warwick, Coventry, CV4 7AL, UK

<sup>3</sup>Wolfson School of Mechanical and Manufacturing Engineering, Loughborough University, Loughborough, LE11 3TU, UK

Tel: (+44) 023 80599450; Fax: (+44) 023 8059 3016; Email: Rong.Jiang@soton.ac.uk

## 1. Introduction:

Powder metallurgy Ni-based superalloys are widely used for aeroengine turbine disc application due to their exceptional strength properties at elevated temperatures, good fatigue and creep performance as well as excellent corrosion and oxidation resistance. However, oxygen enhanced fatigue crack initiation and intergranular propagation at elevated temperatures in air is commonly observed in aeroengine turbine disc superalloys under dwell fatigue testing conditions [1-7], and this phenomenon is usually ascribed to either decohesion/reduction in cohesion strength of grain boundary (GB) due to dynamic embrittlement [8, 9] or GB oxide cracking caused by stress assisted grain boundary oxidation (SAGBO) [5, 10-12]. Although the influence of oxygen on fatigue crack initiation and propagation has been intensively studied, the underlying mechanism for the oxygen-assisted fatigue failure process is still not clear due to the complex composition of disc alloy and the interaction between environmental attack and mechanical load. In this study, fatigue tests were conducted on the Low Solvus, High Refractory (LSHR) alloy designed by NASA for turbine disc application, with a particular focus on studying the influence of the formation of GB oxides on fatigue crack initiation and propagation processes.

## 2. Materials and experimental procedures

The composition (in wt.%) of the LSHR alloy is: 20.7Co, 12.5Cr, 3.5Ti, 3.5Al, 4.3W, 2.7Mo, 1.6Ti, 1.5Nb, 1.5Ta, 0.05Zr, 0.03C, 0.03B, bal. Ni. Fatigue tests were conducted on supersolvus and subsolvus heat treated LSHR alloys (grain size:  $\sim 17.6\mu\text{m}$  and  $\sim 8.1\mu\text{m}$

respectively) under three-point loading at 650 and 725 °C using a trapezoidal 1-1-1-1 waveform (load ratio: 0.1) in combination with a surface replication procedure. The applied load was expected to produce a maximum strain of ~0.8 in the investigated specimens based on finite element simulation. Optical microscopy (OM) and scanning electron microscopy (SEM) were used to evaluate crack evolution. Formation of oxides during fatigue test was assessed by SEM, energy dispersive X-ray spectrometry (EDS) and electron backscatter diffraction (EBSD).

In addition, Oxidation processes at propagating crack tips have been investigated by introducing isotopic  $^{18}\text{O}_2$  during tests under a loading waveform with a 300 second dwell at the peak load (i.e. 1-300-1-1 trapezoidal waveform). The usage of  $^{18}\text{O}_2$  allowed the visualisation of oxygen diffusion paths into the material, and the distribution of  $^{18}\text{O}^-$  was characterised by focussed ion beam (FIB) and secondary ion mass spectrometry (SIMS).

### **3. Results and discussion**

Fatigue lives of the LSHR alloy are shortened by high temperature and high oxygen partial pressure, which are associated with more intergranular fracture mechanisms. Plentiful crack initiation mainly occurs at GBs with bulged GB oxides at elevated temperatures in the LSHR alloy due to oxide cracking. Cracks subsequently propagate along oxidised GBs at surface and exhibit significant crack coalescences at the final stages of fatigue life, as shown in Fig. 1.

Figs.2 (a) and (b) show most of the oxides on the top central surface form at GBs inclined normal to the applied tensile stress, but not all the GBs inclined normal to the tensile stress direction are decorated with bulged oxides, indicating that grain orientation may also influence oxide formation. Bulged GB oxide cracking is indicated by the arrows as shown in Fig.2 (b) along with a close-up showing how cracks propagate along GBs with bulged oxides. Figs.2 (c) and (d) show the concentration variation of Ni, Co, Cr, Ti and Al tracking across GBs with and without bulged oxides analysed by EDS. This qualitative variation of the GB compositional profile indicates that the bulged GB oxides are Co-rich oxide complex, whereas the GBs without bulged oxides are decorated with a Ni/Ti/Al-rich oxide complex.

As shown in Fig.3, it is found that crack paths appear to preferentially locate at the boundaries of high Schmid factor (SF) grain/low SF grain. Similarly, it is found the bulged oxides also tend to form at high SF grain/low SF grain boundaries as indicated by the arrows in Fig. 3 (a) and (c). Figs. 3(d) and (e) shows that the formation of bulged GB oxides is

associated with the difference in SF between grains (as indicated by the arrows), rather than simply a high SF value, as bulged GB oxides are also observed at the boundary of grains with a low SF. The dependence of bulged GB oxide formation on the difference of the SF may indicate that the oxidation process is related to the strain localisation, because dislocations are expected to pile up at boundaries of grains with a large difference in SF as a result of the hindrance of slip transmission at these regions [13, 14]. The distribution of the maximum SF of grains neighbouring the crack paths and in bulk material (Fig. 3 (f)) indicates that the GB oxidation and cracking may not necessarily require a very large difference in SF between neighbouring grains.

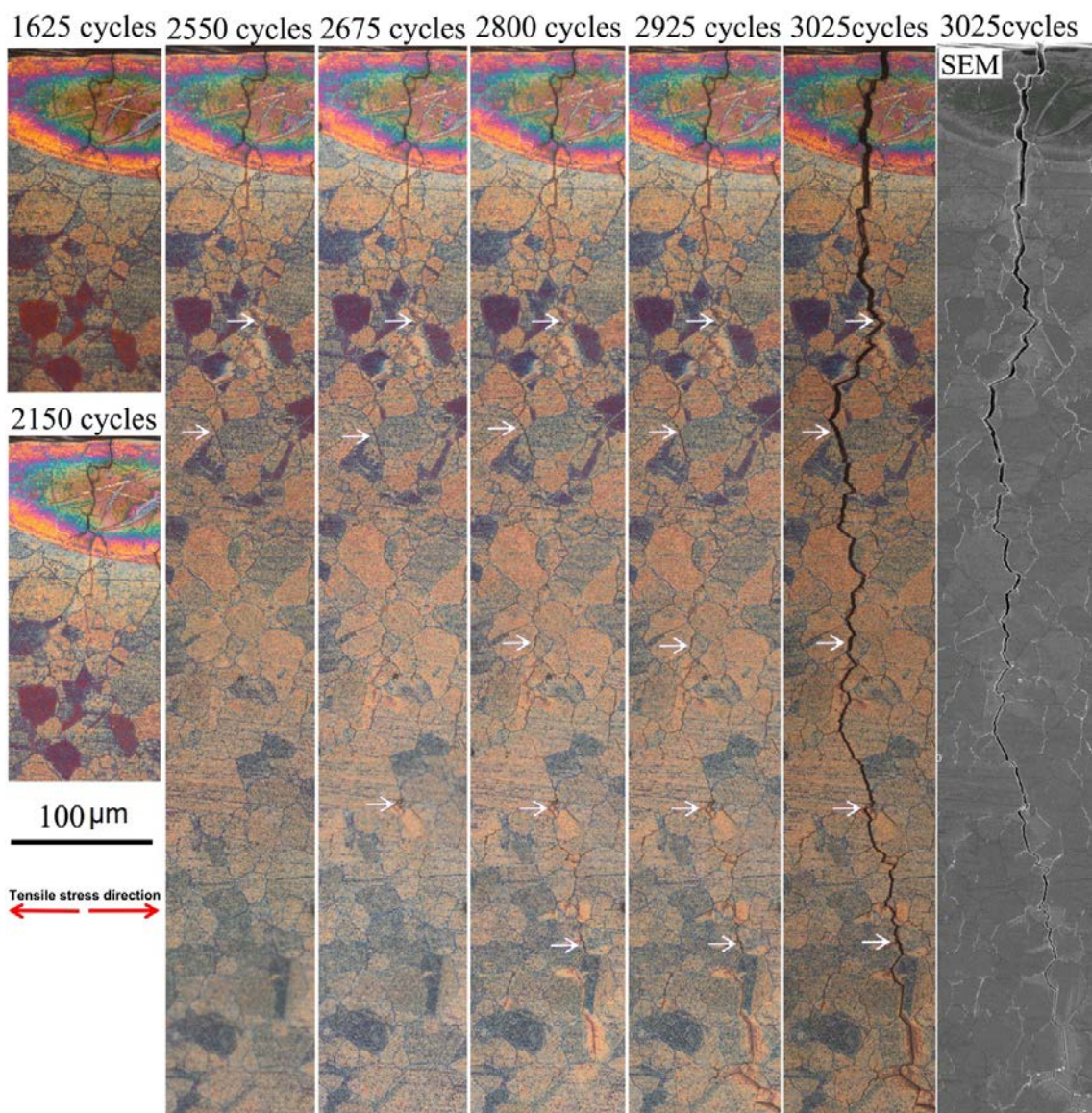


Fig.1 Crack field evolution at the top central surface in the supersolvus heat treated LSHR tested at 650°C. The colouration within the grains is caused by oxidation. The arrows indicate discrete GB oxide cracking.

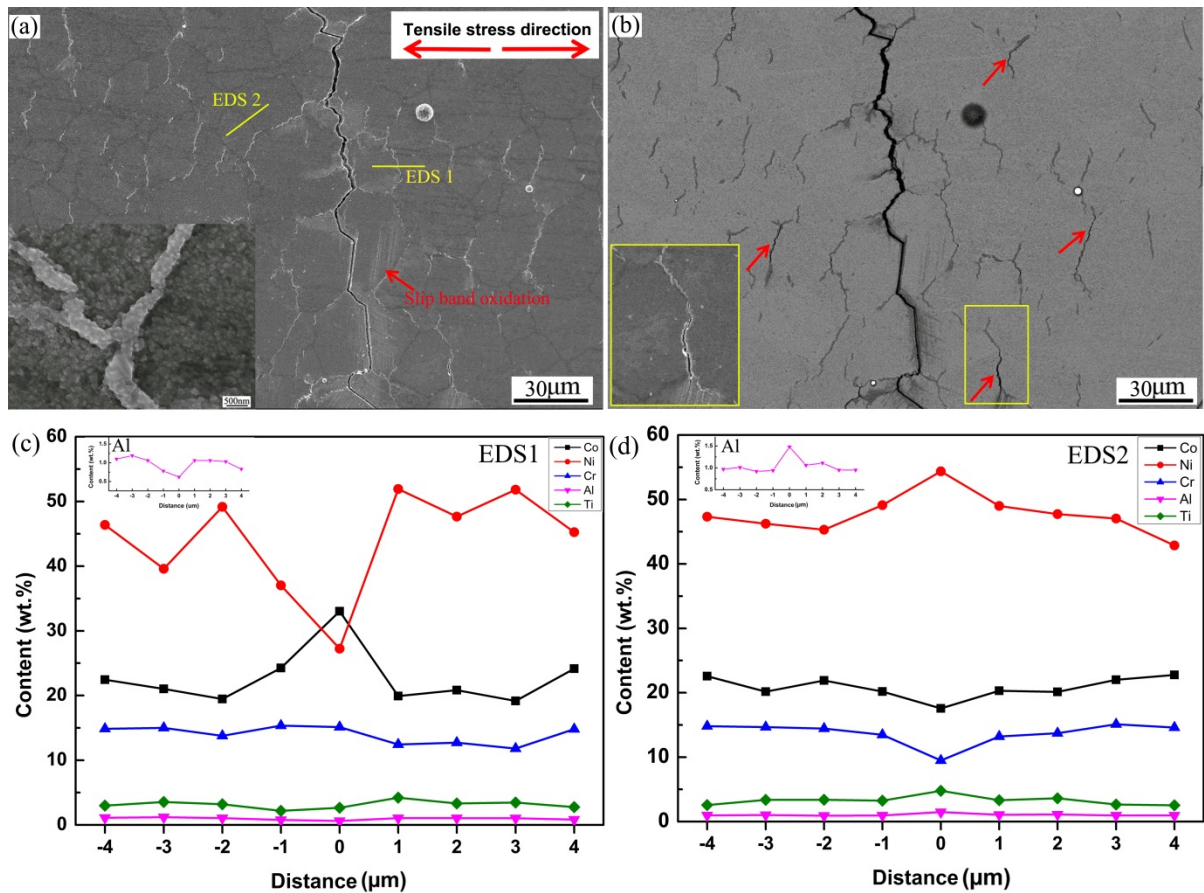


Fig. 2 (a) secondary electron image and (b) backscatter electron image of GB oxidation and cracking in the supersolvus heat treated LSHR alloy tested at 650 °C; compositional profile across grain boundary (c) with bulged oxides and (d) without bulged oxides from EDS analysis. EDS analysis regions are highlighted by yellow lines shown in (a). A close-up of GB bulged oxides is inserted in (a) and a close-up of GB oxide cracking is inserted in (b). The compositional profiles of Al with a rescaled y axis are inserted into (c) and (d) respectively.

Study of oxidation at propagating crack tips indicates that formation of oxides at the crack tip is related to crack propagation rate. When the crack propagation rate is relatively low (at low  $\Delta K$  level), significant oxidation can occur at the crack tip as shown in Fig. 4 where apparent distribution of  $^{18}\text{O}^-$  along grain boundary ahead of the crack tip can be seen. However, limited  $^{18}\text{O}^-$  can be detected for a crack tip with high propagating rate (at high  $\Delta K$  level).



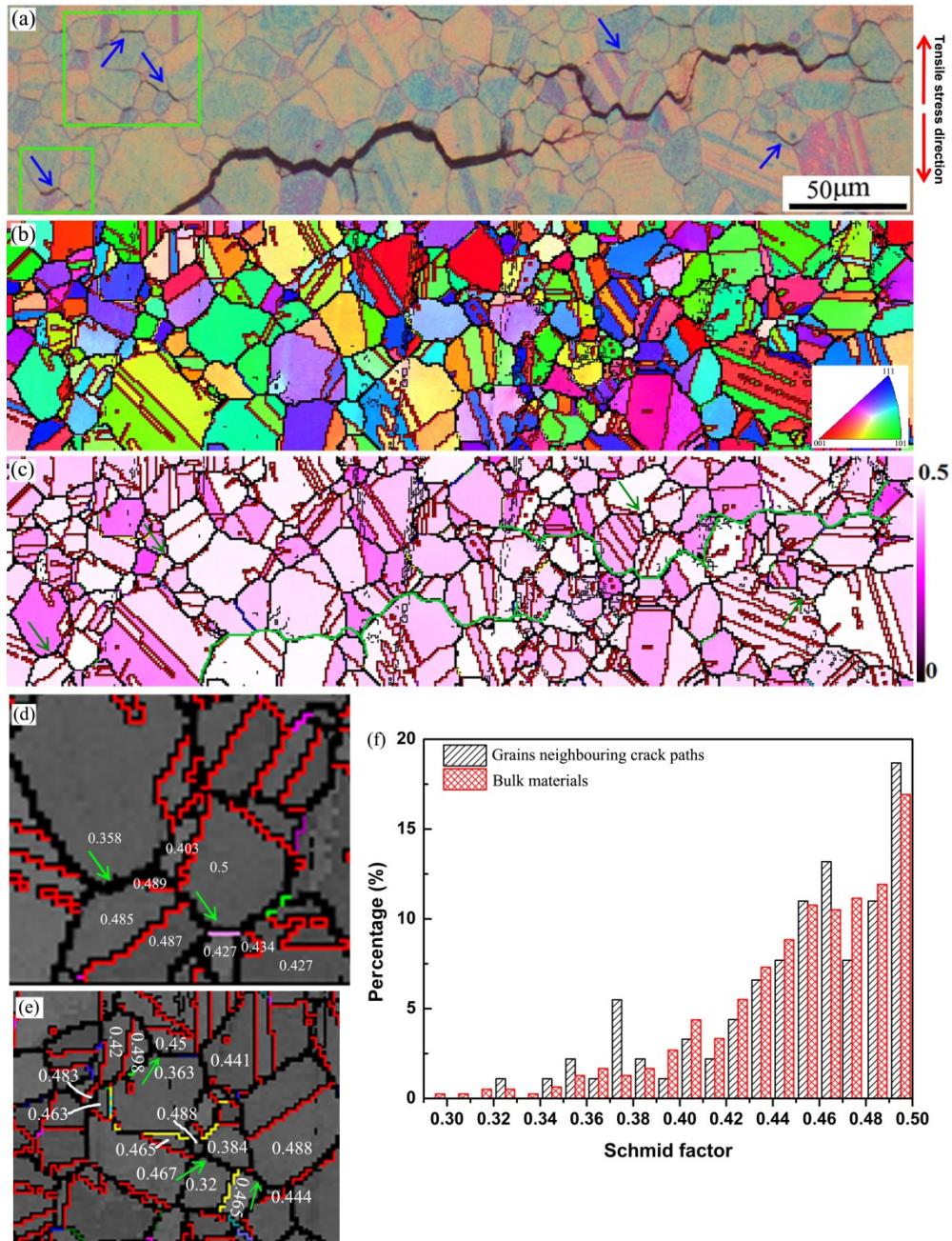


Fig.3 (a) Morphology of GB oxidation and cracking in the supersolvus heat treated LSHR alloy tested at 650 °C observed under OM; (b) grain orientation map; (c) colour-coded SF map of the region shown in (a), crack paths are outlined on the SF map by green lines; (d) and (e) maximum SF of the grains of interest highlighted at the bottom and top shown in (a) respectively, the GBs with bulged oxides are indicated by the green arrows; and (f) SF distribution of grains neighbouring the crack paths and bulk materials.

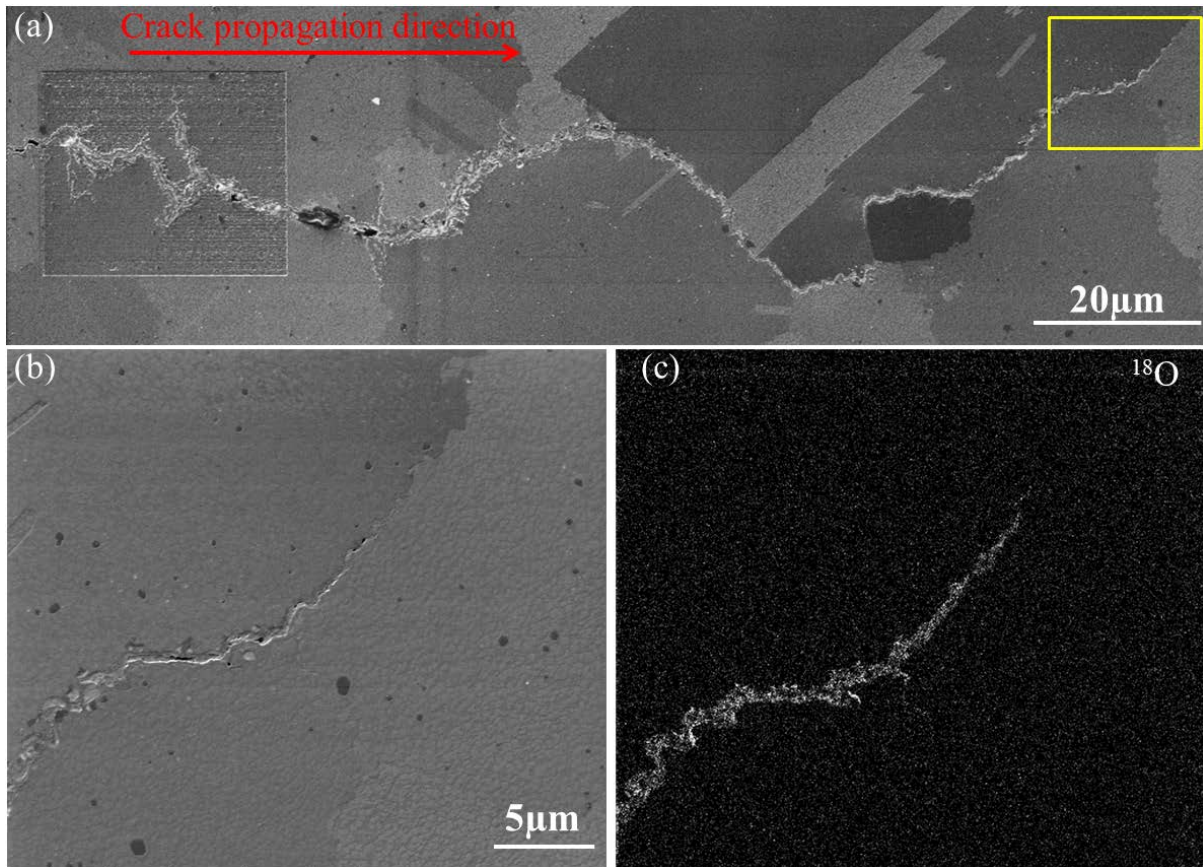


Fig. 4 Oxidation in a propagating crack tip in the supersolvus heat treated LSHR tested at 725 °C: (a) overview of the crack tip, (b) close-up of the crack tip highlighted in (a), and (c) distribution of  $^{18}\text{O}$  at the crack tip.

#### 4. Conclusions

Plentiful crack initiation mainly occurs at bulged GB Co-rich oxide complexes at elevated temperatures in the LSHR alloy due to oxide cracking. Cracks subsequently propagate along oxidised GBs and exhibit significant crack coalescence at the final stages of fatigue life. Formation of bulged GB Co-rich oxide complexes is closely related to the strain localisation which is associated with grain orientation and applied stress. The boundaries of high SF grain/low SF grain are preferential site for formation of bulged Co-rich oxide complexes. Oxidation at propagating crack tips is closely related to the crack propagation rate. The oxidation process is significant when crack propagation rate is low, but this oxidation process can be suppressed to an insignificant level when cracks propagate fast at high  $\Delta K$  level.

## Acknowledgement

Thanks are due to the EPSRC (Grant EP/K027271/1) of the UK and China Scholarship Council for funding support, and to NASA of US for the supply of the LSHR alloys.

## References

- [1] S. Everitt, R. Jiang, N. Gao, M. J. Starink, J. W. Brooks and P. A. S. Reed, *Materials Science and Technology*, 29 (2013) 781-787.
- [2] H.T. Pang, P. A. S. Reed, *Materials Science and Engineering: A*, 448 (2007) 67-79.
- [3] R. Molins, G. Hochstetter, J. C. Chassigne, E. Andrieu, *Acta Materialia*, 45 (1997) 663-674.
- [4] J. Tong, J. Byrne, *Fatigue & Fracture of Engineering Materials & Structures*, 22 (1999) 185-193.
- [5] L. Ma, K.-M. Chang, *Scripta Materialia*, 48 (2003) 1271-1276.
- [6] T. P. Gabb, J. Gayda, J. Telesman, L. J. Ghosn, A. Garg, *International Journal of Fatigue*, 48 (2013) 55-67.
- [7] R. Jiang, S. Everitt, M. Lewandowski, N. Gao, P.A.S. Reed, *International Journal of Fatigue*, 62 (2014) 217-227.
- [8] U. Krupp, W. M. Kane, C. Laird, C. J. McMahon, *Materials Science and Engineering: A*, 387-389 (2004) 409-413.
- [9] J. A. Pfaendtner, C. J. McMahon Jr, *Acta Materialia*, 49 (2001) 3369-3377.
- [10] E. Andrieu, R. Molins, H. Ghonem, A. Pineau, *Materials Science and Engineering: A*, 154 (1992) 21-28.
- [11] C. F. Miller, G. W. Simmons, R. P. Wei, *Scripta Materialia*, 48 (2003) 103-108.
- [12] H. S. Kitaguchi, H. Y. Li, H. E. Evans, R. G. Ding, I. P. Jones, G. Baxter, P. Bowen, *Acta Materialia*, 61 (2013) 1968-1981.
- [13] W. Z. Abuzaid, M. D. Sangid, J. D. Carroll, H. Sehitoglu, J. Lambros, *Journal of the Mechanics and Physics of Solids*, 60 (2012) 1201-1220.
- [14] Z. J. Zhang, P. Zhang, L. L. Li, Z. F. Zhang, *Acta Materialia*, 60 (2012) 3113-3127.